

Chemical mixing and hard mode spectroscopy in ferroelastic lead phosphate arsenate: local symmetry splitting and multiscaling behaviour

This article has been downloaded from IOPscience. Please scroll down to see the full text article.

2010 J. Phys.: Condens. Matter 22 045403

(<http://iopscience.iop.org/0953-8984/22/4/045403>)

View [the table of contents for this issue](#), or go to the [journal homepage](#) for more

Download details:

IP Address: 129.252.86.83

The article was downloaded on 30/05/2010 at 06:38

Please note that [terms and conditions apply](#).

Chemical mixing and hard mode spectroscopy in ferroelastic lead phosphate arsenate: local symmetry splitting and multiscaling behaviour

E K H Salje^{1,3}, T Beirau², B Mihailova^{2,3}, T Malcherek² and U Bismayer²

¹ Department of Earth Sciences, University of Cambridge, Downing Street, Cambridge CB2 3EQ, UK

² Department Geowissenschaften, Universität Hamburg, Grindelallee 48, D-20146 Hamburg, Germany

E-mail: ekhard@esc.cam.ac.uk and boriana.mihailova@uni-hamburg.de

Received 3 November 2009, in final form 28 November 2009

Published 12 January 2010

Online at stacks.iop.org/JPhysCM/22/045403

Abstract

The phase transition in ferroelastic $\text{Pb}_3(\text{PO}_4)_2\text{-Pb}_3(\text{AsO}_4)_2$ mixed crystals shows typical multiscaling behaviour with two relevant length and timescales. One length scale is macroscopic and shows uniform, weakly first-order phase transitions between a rhombohedral paraphase ($R\bar{3}m$) and a monoclinic ferroelastic phase ($C2/c$). The second length scale is on the level of tetrahedral complexes which display monoclinic distortions at temperatures well above the macroscopic transition point. For instance, in $\text{Pb}_3(\text{P}_{0.43}\text{As}_{0.57}\text{O}_4)_2$ the AsO_4 polyhedra show static deformation up to ~ 60 K above the deformation of the PO_4 tetrahedra. The two timescales are either short compared with the time of observation, namely the dynamic reorientation of the PO_4 tetrahedral distortion, or very long. The long timescale refers then to the (quasi)static distortion of the AsO_4 tetrahedra which persists at $T > T_c$. These distortions appear to be uncorrelated or only weakly correlated and their random field leads to an order/disorder aspect of the phase transition which remains, on a phonon timescale, essentially displacive in character.

(Some figures in this article are in colour only in the electronic version)

1. Introduction

Lead phosphate and its arsenate derivatives, lead phosphate arsenate, are examples for multiscale behaviour of ferroelastic phase transitions. The phase transition from the rhombohedral to the monoclinic phase $R\bar{3}m\text{-}C2/c$ at 456 K is essentially displacive in character, with a soft mode excitation near 40 cm^{-1} at room temperature [1–4]. In addition, an order-disorder component exists [5, 6]. Its dynamical excitation is related to the reorientation of the twofold axis of symmetry (diad) perpendicular to the threefold axis (triad) in the rhombohedral $R\bar{3}m$ structure. It was shown that this order-

disorder component is well described by a three-state Potts model [6] where the iso-spin is related to the deviation of the Pb position from the triad. The dynamic movement is then the discontinuous rotation around the triad at high temperatures. The rhombohedral symmetry is hence the result of time and space averaging on a macroscopic scale. Each orientation of the Pb position along a diad represents a domain configuration at $T < T_c$. The displacive character of the transition stems from the amplitude of the off-centring of Pb which disappears at sufficiently high temperatures so that the rotational aspect becomes inoperative [7–11].

The interplay of the displacive off-centring and the iso-spin behaviour of the orientation disorder of the Pb position was investigated in great detail in $\text{Pb}_3(\text{PO}_4)_2$. Two major

³ Authors to whom any correspondence should be addressed.

results were that the disorder is purely dynamic and is strong between 433 and 523 K while the macroscopic phase transition occurs at 456 K. The phase transition is slightly first order so that the experimental determination of the transition temperature and T_c is unequivocal. The excitation of the order/disorder component, the flip mode, has a characteristic frequency of 3×10^{10} Hz [3].

The flip mode has a static component once the material is doped with As. The characteristic length over which ordered regions establish themselves is above 3 nm in pure lead phosphate and larger in mixed crystals [2, 7]. The question then arises: what happens when the doping level becomes large and mixed crystals are formed. More precisely, does the characteristic length scale diverge and what happens to the dynamical excitation of the flip mode in the monoclinic phase?

This question has wider implications for the analysis of chemical mixing in general. Let us first assume ideal mixing (on any length scale): the displacive transition remains in this case a homogeneous feature besides the obvious thermodynamic fluctuations of the order parameter. In this scenario we find that the transition temperature is a single-valued function of the composition. The lowest transition temperature occurs at the lowest value of the effective interaction parameter or, in a soft mode picture, at the composition where the soft mode is most stable. This condition is met if the most stable configurations are given by the two end members of the series of mixed crystals. Such ideal mixing is not encountered in $\text{Pb}_3(\text{PO}_4)_2$ – $\text{Pb}_3(\text{AsO}_4)_2$, however. The most stable configuration of the rhombohedral phase is near the 50–50 mixture of phosphate and arsenate groups; this composition has the lowest transition temperature. The phase diagram then shows an almost linear mixing curve of the transition temperature between the two chemical end members and the 50–50 composition which takes on the role of a new ‘end member’ of the mixing behaviour. The phase diagram is effectively split into two parts, namely the P-rich compounds for one part of the mixing behaviour and the As-rich compounds for the other [3, 7].

These observations beg the question of how the effective ‘end-member’ phase $\text{Pb}_3(\text{P}_{0.5}\text{As}_{0.5}\text{O}_3)_2$ is characterized on a local, atomic scale. The ideal experimental tool for such investigations is ‘hard mode spectroscopy’ where the frequency shift of high frequency optical phonons is correlated with the structural order parameter [12–18]. The theoretical expectation and the experimental evidence is that the change of frequency ω is

$$(\Delta\omega^2) \sim Aq^2 + Bq^4$$

where ω is the hard mode frequency with $(\Delta\omega^2) = \omega^2 - \omega_0^2 \sim 2\omega_0(\omega - \omega_0) = 2\omega_0\delta\omega$ and $A \gg B$ for most compounds; q is the state parameter on a local scale which, after averaging, relates to the thermodynamic order parameter Q (see [19] for the discussion of domain boundaries). The characteristic length scale of hard mode spectroscopy was determined in detail [12, 18] and is for high frequency phonons of less than a lattice unit in $\text{Pb}_3(\text{PO}_4)_2$. The results of the hard mode spectroscopy can then be compared

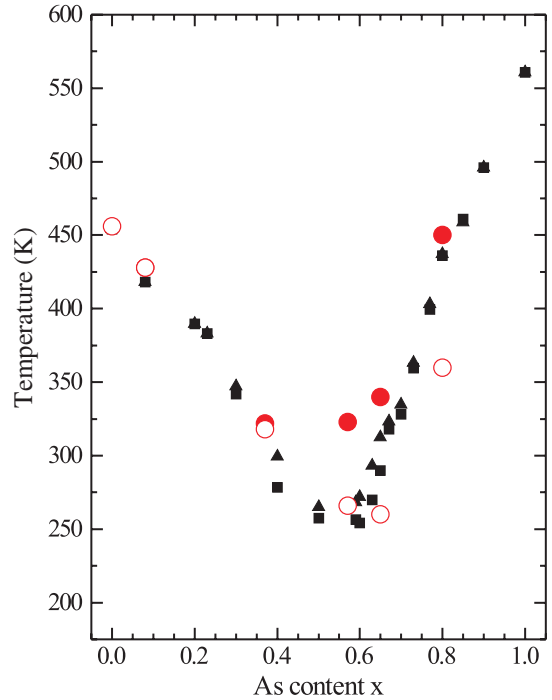


Figure 1. Phase transition temperature T_c (triangles) and the temperature of discontinuity in the optical birefringence (squares) as a function of the As content x along with the highest temperature at which the splitting of the Raman scattering arising from AsO_4 (filled circles) and PO_4 bending modes (open circles) is resolved.

with macroscopic measurements of the order parameter Q using optical birefringence [2], diffraction techniques [11] or measurements of the specific heat of the transition [4]. All transition temperatures would coincide in uniform materials while every deviation is a signature for spatial and/or temporal heterogeneity and multiscaling behaviour.

2. Experimental details

Optically homogeneous single crystals of $\text{Pb}_3(\text{P}_{1-x}\text{As}_x\text{O}_4)_2$ were grown by the Czochralski technique [2]. The chemical compositions of the single-crystal samples were determined by electron microprobe analysis (Camebax microbeam SEM system) and a spatial average over 50 positions was taken for each compound. The chemical compositions of the crystals were found to be close to the corresponding nominal compositions. The overall chemical homogeneity of the samples was additionally verified by backscattering electron imaging. Following the phase diagram in figure 1 [2], we have chosen single crystals with $x = 0, 0.08, 0.37, 0.57, 0.65$ and 0.80 .

Raman scattering at 514.5 nm was performed using a Horiba Jobin-Yvon T64000 triple-grating spectrometer equipped with an Olympus BX4 microscope. Unpolarized spectra were collected in backscattering geometry from plate-like specimens with the cleavage plane (monoclinic (b, c) or rhombohedral (a, b)) perpendicular to the direction of the incident light. The spectral resolution was approximately 1.5 cm^{-1} . Temperature-dependent Raman

scattering experiments were conducted using a Linkam heating/cooling stage. Data were recorded from 80 to 600 K with a heating rate of 10 K min^{-1} . The uncertainty in the temperature determination was 0.1 K. The reversibility and repeatability of the observed spectral changes were verified by collecting Raman scattering data on heating and cooling and from at least two different spatial single-domain regions for each compound. For narrow temperature ranges close to the detected characteristic temperatures additional runs with smaller heating/cooling rates were conducted to double check the narrow temperature hysteresis ($\leq 1 \text{ K}$) of structural changes. The latter is in full accordance with the hysteresis of 0.4 K determined by optical birefringence measurements on $\text{Pb}_3(\text{PO}_4)_2$ [20] and with the heat capacity behaviour of mixed $\text{Pb}_3(\text{P}_{1-x}\text{As}_x\text{O}_4)_2$ [4], corresponding to a weak discontinuous transition with a very narrow hysteresis.

The measured spectra were subsequently normalized to account for the Bose–Einstein occupation factor. The peak positions, full widths at half-maxima (FWHMs) and the integrated intensities were determined by fitting the spectral profiles with Lorentzian functions as a good approximation for underdamped oscillators.

3. Results and discussion

Figures 2 and 3 show Raman spectra of $\text{Pb}_3(\text{P}_{1-x}\text{As}_x\text{O}_4)_2$ as a function of temperature. Spectra measured at temperatures approx. 100 K above and below the phase transition temperature T_c are compiled in figure 2. Analysis of the fitted line profiles shows that the tetrahedral modes of $\text{Pb}_3(\text{P}_{1-x}\text{As}_x\text{O}_4)_2$ mixed crystals exhibit a typical two-mode behaviour within the entire range of concentration x . The stretching and bending modes of PO_4 and AsO_4 tetrahedra are energetically well separated [21–27]. The temperature evolution of the Raman scattering below 500 cm^{-1} relates to lattice modes and shows a continuous dependence on the chemical composition. The splitting of the modes can now be compared with the macroscopic transition temperatures [2] for $x = 0, 0.08, 0.37, 0.57, 0.65$ and 0.80 which are 456, 420, 315, 265, 330 and 440 K, respectively. The structural phase transitions were found to occur at slightly higher temperatures than the onset of peak splitting in compounds with high P content ($x = 0, 0.08$ and 0.37). For the end-member composition $\text{Pb}_3(\text{PO}_4)_2$ the shape of the peak generated by the antisymmetric tetrahedral bending mode is particularly sensitive to the development of a static monoclinic phase. The monoclinic splitting of this peak appears on cooling very close to the macroscopically observed transition temperature at 456 K. This can be contrasted with the dynamic flip mode which is seen as a broadening of the 80 cm^{-1} mode [3] and occurs between 433 K and $T \gg T_c$. Similar anomalies such as the appearance of the flip mode are seen in the lattice spacings [11] and excess specific heat of the transition [4].

For $x = 0.08$ and 0.37 the splitting of the AsO_4 bending mode occurs at the same temperature (within experimental uncertainties) as that of the PO_4 bending mode. In contrast, we observe that the equivalent phonons behave very differently in As-rich compounds ($x = 0.57, 0.65$ and 0.80). The arsenate

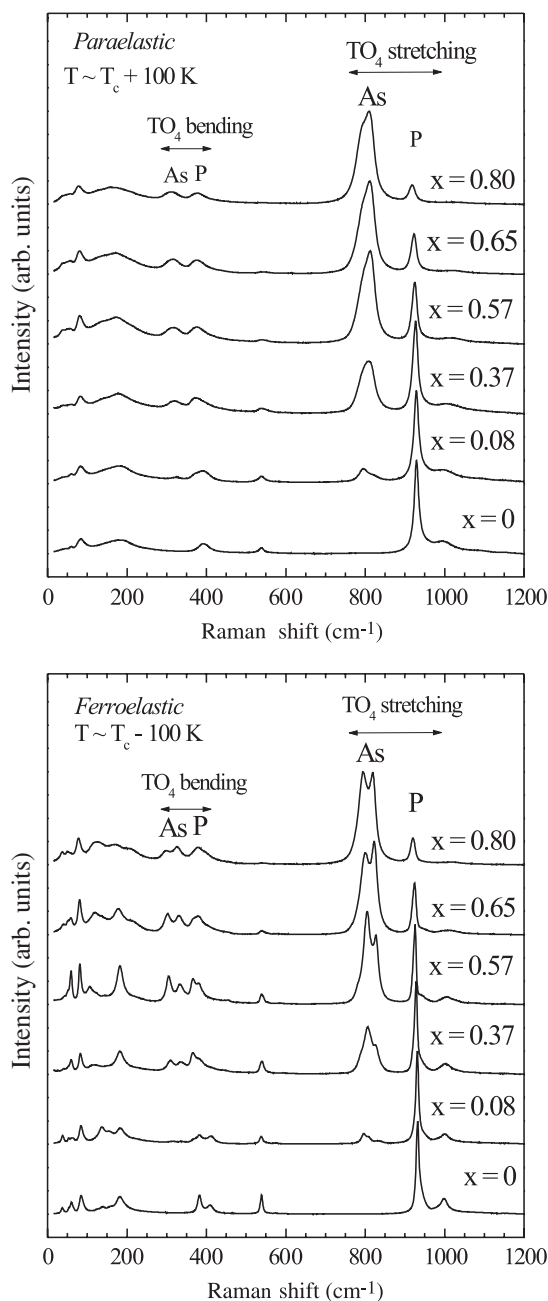


Figure 2. Raman spectra of $\text{Pb}_3(\text{P}_{1-x}\text{As}_x\text{O}_4)_2$ measured at $\sim 100 \text{ K}$ above the transition temperature T_c (upper plot) and at $\sim 100 \text{ K}$ below T_c (bottom plot); $T_c = 456, 420, 315, 265, 330$ and 430 K for $x = 0, 0.08, 0.37, 0.57, 0.65$ and 0.80 , respectively.

and the phosphate tetrahedral groups show peak splittings at two different temperatures. For $x = 0.65$ and 0.80 the splitting of the AsO_4 bending mode occurs close to the macroscopic transition point while the equivalent peak splitting of the phosphate modes occurs at lower temperatures (figure 1).

We now focus on the transition mechanism for $\text{Pb}_3(\text{P}_{1-x}\text{As}_x\text{O}_4)_2$ with $x = 0.57$, which was identified as being close to the composition of the end member of the two series of mixed crystals ($0 < x < 0.5$ and $0.5 < x < 1$). Cooling the sample from high temperatures to $\sim 320 \text{ K}$ leads to a local deformation of the AsO_4

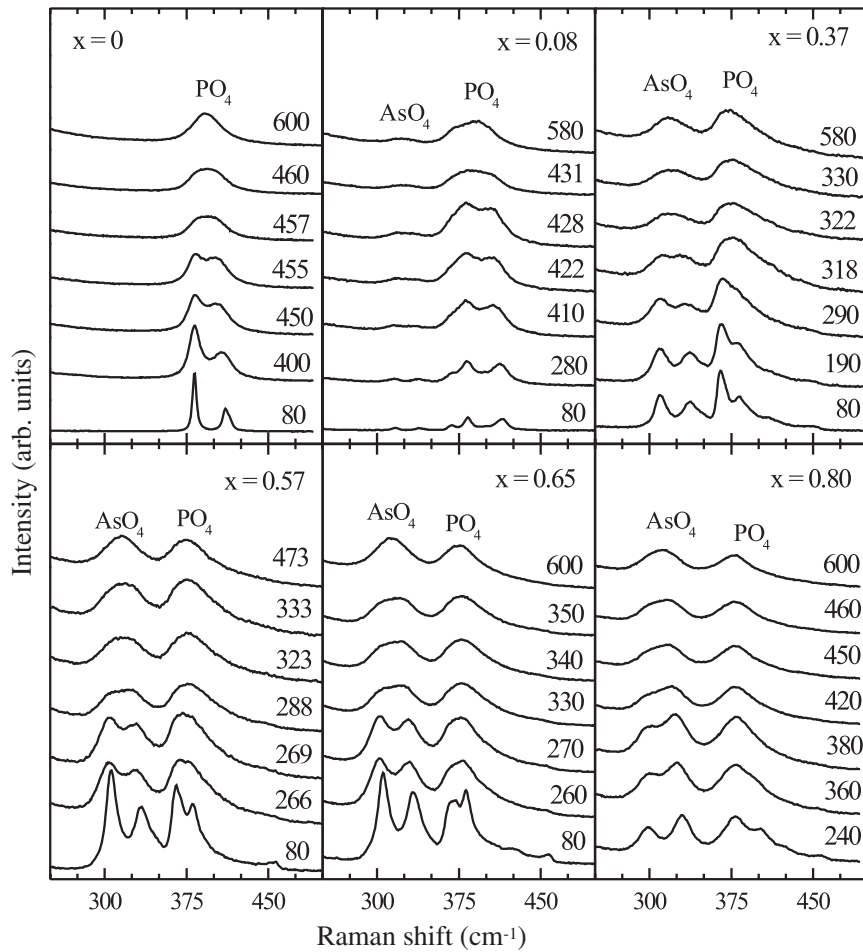


Figure 3. Selected Raman spectra of $\text{Pb}_3(\text{P}_{1-x}\text{As}_x\text{O}_4)_2$ in the spectral range $250\text{--}500\text{ cm}^{-1}$ arising from TO_4 bending modes. Temperatures (K) are indicated for each trace. The transition temperature T_c and the temperatures of the onset of splitting $T_{\text{PO}_4}^{\text{split}}$ and $T_{\text{AsO}_4}^{\text{split}}$ (bending modes) are $T_c = 456, 420, 315, 265, 330$ and 430 K; $T_{\text{PO}_4}^{\text{split}} = 456, 428, 318, 266, 260$ and 360 K; and $T_{\text{AsO}_4}^{\text{split}} = \text{n.a.}, 428, 322, 323, 340$ and 450 K for $x = 0, 0.08, 0.37, 0.57, 0.65$ and 0.80 , respectively.

tetrahedron which adopts the monoclinic symmetry as seen by the peak splitting of the relevant bending mode. The PO_4 bending mode does not change at this temperature so that we conclude that the tetrahedron remains rhombohedral on the timescale of the experiment. The PO_4 tetrahedron becomes monoclinic (quasi)statically near 265 K at which temperature the macroscopic spontaneous strain is established and the crystal transforms to the monoclinic state on a macroscopic length and timescale. This transition is weakly first order so that there is no experimental uncertainty about the transition temperature besides the effect of a small temperature hysteresis.

The understanding of the interval between 265 and 320 K is hence crucial for the description of the transition mechanism. The dynamical excitation above the static transition temperature in $\text{Pb}_3(\text{PO}_4)_2$ is the flip mode which is observed by Raman spectroscopy between approx. $T = 433$ K and $T_c + 100$ K [3]. As-doped material shows a static local deformation over a similar temperature interval. The same picture emerges from our measurements: both tetrahedral complexes show deviations from the high symmetry form but only the AsO_4 tetrahedron displays a static deformation while

the deformation in PO_4 is dynamic even in the presence of static AsO_4 deformations. This is the first time that precursor ordering in one and the same crystal is shown experimentally to be different for two different chemical complexes: dynamic in PO_4 and static in AsO_4 [28].

The highest resolution for the transition process is obtained when data are analysed using the autocorrelation method [29–31]. This method analyses the correlation of the spectrum with itself:

$$A(\omega) = \int_{-\infty}^{\infty} f(\omega') f(\omega - \omega') d\omega'$$

and is particularly sensitive to small changes in the linewidths and peak splittings. Figure 4 shows the temperature evolution of the autocorrelation function Δcorr for $x = 0.57$ of the bands $740\text{--}886\text{ cm}^{-1}$ (AsO_4 stretching) and $886\text{--}973\text{ cm}^{-1}$ (PO_4 stretching) [29].

The temperature dependence of the width Δcorr of the fitted central component of the autocorrelation function for both bands shows an anomaly near 265 K, which corresponds to the macroscopic ferroelastic transition temperature of the sample, namely where the optical birefringence completely

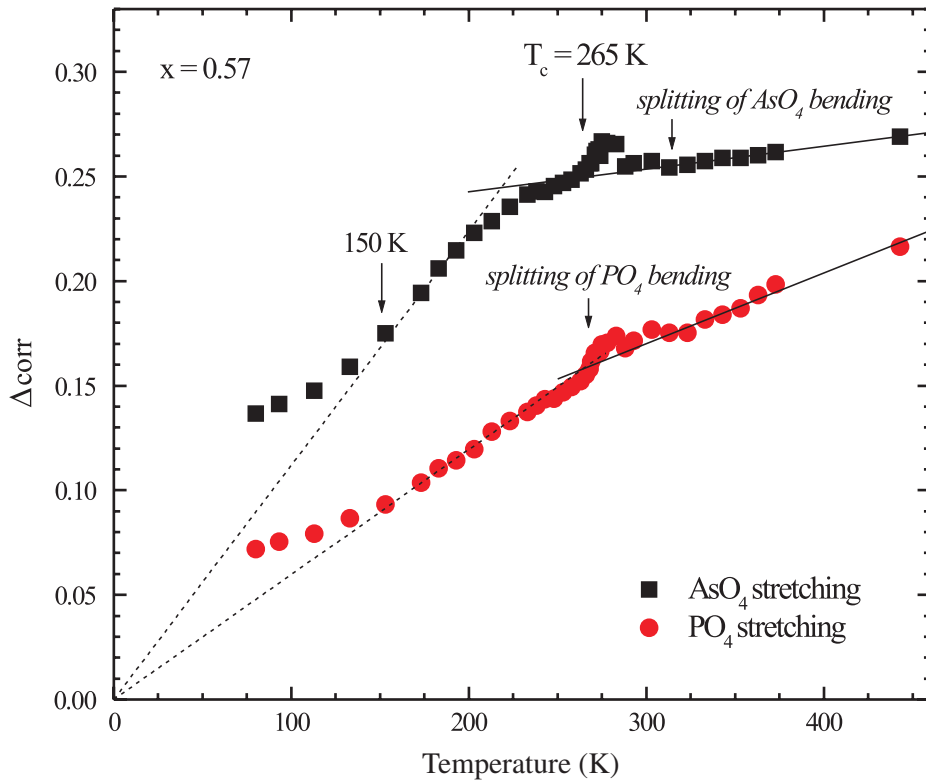


Figure 4. Temperature dependence of the autocorrelation Δcorr of $\text{Pb}_3(\text{P}_{0.43}\text{As}_{0.57}\text{O}_4)_2$ calculated for the band generated by AsO_4 stretching modes (squares) and for the band generated by PO_4 stretching modes (circles). The macroscopically determined T_c is 265 K; the splitting of the peak arising from AsO_4 bending modes is resolved at ~ 323 K, while that of the peak arising from PO_4 bending modes at $\sim T_c$. The dashed lines represent linear fits $y(x) = bx$ through the experimental points between 153 and 203 K. Below 150 K weak anharmonicities are shown by saturation of the linewidth. The solid lines represent linear fits $y(x) = a + bx$ through the experimental points above 323 K. The ‘peak’ of the autocorrelation function at $T > T_c$ is related to the dynamical flip mode while the additional static disorder of the AsO_4 tetrahedra shows only a very small stepwise increase of Δcorr .

disappears on heating. The collapse of the structure occurs at slightly lower temperatures [2, 3]. At higher temperatures a line broadening is visible until 275 K, which is similar to the anomaly in pure $\text{Pb}_3(\text{PO}_4)_2$ where the broadening was identified as due to the dynamical behaviour of the flip mode. The additional broadening or line splitting remains until above 300 K which is related to the splitting of the AsO_4 modes and shows that this tetrahedron has not reached rhombohedral symmetry until temperatures much above the macroscopic transition point.

The autocorrelation analysis also shows deviations from linear temperature dependence near 150 K, below which temperature the additional line splitting or residual broadening of the Raman line appears, showing ‘anharmonicity’ or weak line splitting due to local symmetry breaking. Nevertheless, the rapid decay of the autocorrelation function at low temperatures shows that the transition has a very strong displacive component and that dynamical flip mode excitations are relevant only near the transition point.

4. Conclusion

The phase transition of $\text{Pb}_3(\text{P}_{1-x}\text{As}_x\text{O}_4)_2$ is characterized by two lines of non-ideal mixing: one between the PO_4 end member and a composition near the 50–50 mixture, the second between this composition and the AsO_4 end member.

The transition temperature is a nonlinear function of the composition because the plateau effect is valid near the 50–50 composition while an inverse plateau exists at either chemical end member [31–36]. The transitions are essentially displacive but display an additional order–disorder component near the transition points. This order–disorder component has different consequences for the PO_4 and AsO_4 tetrahedra on a phonon timescale: while the rotation of the twofold axis, i.e. the flip mode, remains dynamic over a small temperature interval for the PO_4 tetrahedra, we find that the AsO_4 shows ‘static’ monoclinic distortions even on an atomistic length scale. Similar AsO_4 distortions have been observed in KDP-type compounds by NMR [37] and shown to be dynamic at longer timescales of the NMR experiments. In this paper we can only comment on the phonon timescale while we do not know whether orientational disorder exists on a 10^{-6} s timescale, as was extrapolated in CsH_2AsO_4 [38]. The tendency to reduce the transition temperature for mixed compounds was also seen in $\text{KH}_2(\text{P}_{1-x}\text{As}_x)\text{O}_4$ where similar local distortions can be expected [39].

Acknowledgments

UB and BM are indebted to the Deutsche Forschungsgemeinschaft (INST 152/485-1 FUGG). EKHS is grateful to the Alexander von Humboldt Foundation for a travel grant.

References

- [1] Brixner L N, Biersted P E and Jaep W F 1973 *Mater. Res. Bull.* **8** 497
- [2] Bismayer U and Salje E 1981 *Acta Crystallogr. A* **37** 145
- [3] Salje E, Devarajan V, Bismayer U and Guimaraes D M C 1983 *J. Phys. C: Solid State Phys.* **16** 5233
- [4] Salje E and Wruck B 1983 *Phys. Rev. B* **28** 6510
- [5] Kiat J M, Calvarin G and Yamada Y 1993 *Phys. Rev. B* **48** 34
Nepochatenko V A and Dudnik E F 2003 *Phys. Solid State* **45** 1966
- [6] Salje E and Devarajan V 1981 *J. Phys. C: Solid State Phys.* **14** 1029
- [7] Bismayer U, Salje E and Joffrin C 1982 *J. Physique* **43** 1379
Cho Y C, Lee H J, Park S E, Cho C R and Jeong S Y 2002 *Phys. Rev. B* **66** 184103
- [8] Wruck B, Salje E K H, Zhang M, Abraham T and Bismayer U 1994 *Phase Transit.* **48** 135
Parlinski K and Kawazoe Y 1997 *J. Mater. Res.* **12** 2366
- [9] Wruck B, Bismayer U and Salje E 1981 *Mater. Res. Bull.* **16** 251
- [10] Bismayer U, Mathes D, Bosbach D, Putnis A, van Tendeloo G, Novak J and Salje E K H 2000 *Mineral. Mag.* **64** 233
- [11] Salje E K H, Graeme-Barber A, Carpenter M A and Bismayer U 1993 *Acta Crystallogr. B* **49** 387
Mori S, Yamamoto N, Koyama Y, Uesu Y and Yamada Y 1994 *Trans. Mater. Res. Soc. Japan* **18** 885
- [12] Salje E K H and Bismayer U 1997 *Phase Transit.* **63** 1
- [13] Ballaran T B, Carpenter M A, Domeneghetti C, Salje E K H and Tazzoli V 1998 *Am. Mineral.* **83** 434
Zhang M, Salje E K H, Bismayer U, Unruh H G, Wruck B and Schmidt C 1995 *Phys. Chem. Miner.* **22** 41
Salje E K H, Zhang M and Zhang H L 2009 *J. Phys.: Condens. Matter* **33** 335402
- [14] Bismayer U 2000 *Rev. Mineral. Geochem.* **39** 265
Bismayer U 1990 *Phase Transit.* **27** 211
- [15] Atkinson A J, Carpenter M A and Salje E K H 1999 *Eur. J. Mineral.* **11** 7
- [16] Zhang M, Wruck B, Barber A G, Salje E K H and Carpenter M A 1996 *Am. Mineral.* **81** 92
- [17] Meyer H W, Carpenter M A, Becerro A I and Seifert F 2002 *Am. Mineral.* **87** 1291
- [18] Salje E K H 1992 *Phase Transit.* **37** 83
- [19] Salje E and Zhang H L 2009 *Phase Transit.* **82** 452
- [20] Wood I G, Wadhawan V K and Glazer A M 1980 *J. Phys. C: Solid State Phys.* **13** 5155
- [21] Chang I F and Mitra S S 1971 *Adv. Phys.* **20** 359
- [22] Prabukanthan P and Dhanasekaran R 2008 *J. Phys. D: Appl. Phys.* **41** 115102
- [23] Pages O, Tite T, Kim K, Graf P A, Maksimov O and Tamargo M C 2006 *J. Phys.: Condens. Matter* **18** 577
- [24] Romcevic N, Golubovic A, Romcevic M, Trajic J, Nikolic S, Duric S and Nikiforov V N 2005 *J. Alloys Compounds* **402** 36
- [25] Xu C M, Huang W H, Xu J, Yang X J, Zuo J, Xu X L and Liu H T 2004 *J. Phys.: Condens. Matter* **16** 4149
- [26] Podobedov V B, Weber A, Romero D B, Rice J P and Drew H D 1998 *Solid State Commun.* **105** 589
- [27] Bismayer U, Hensler J, Salje E and Güttler B 1994 *Phase Transit.* **48** 149
- [28] Salje E K H 2008 *J. Phys.: Condens. Matter* **20** 485003
- [29] Salje E K H, Carpenter M A, Malcherek T and Ballaran T B 2000 *Eur. J. Mineral.* **12** 503
- [30] Rodehorst U, Carpenter M A, Marion S and Henderson C M B 2003 *Mineral. Mag.* **67** 989
Salje E K H, Ridgwell A, Güttler B, Wruck B, Dove M T and Dolino G 1992 *J. Phys.: Condens. Matter* **4** 571
- [31] Tarantino S C, Carpenter M A and Domeneghetti M C 2003 *Phys. Chem. Mineral.* **30** 495
- [32] Hayward S A and Salje E K H 1996 *Am. Mineral.* **81** 1332
- [33] Salje E K H 1995 *Eur. J. Mineral.* **7** 791
- [34] Salje E, Bismayer U, Wruck B and Hensler J 1991 *Phase Transit.* **35** 61
- [35] Kim K W, Kim T S, Jeon M K, Oh K S, Jung C H and Woo S I 2008 *Appl. Phys. Lett.* **92** 052911
- [36] Rasmussen S B, Hamma H, Lapina O B, Khabibulin D F, Eriksen K M, Berg R W, Hatem G and Fehrmann R 2003 *J. Phys. Chem. B* **107** 13823
- [37] Blinc R, Cevc P and Cevc G 1979 *J. Chem. Phys.* **70** 153
- [38] Kahol P K, Scoular D T and Dalal N S 1991 *J. Phys.: Condens. Matter* **3** 6635
- [39] Lee K S, Ju S M and Kim J B 1994 *Phys. Rev. B* **49** 9958